Attractors for flow observables in $2 + 1$D Bjorken flow

Victor E. Ambruș[1], Clemens Werthmann[2], Sören Schlichting[2]

[1] Physics Faculty, West University of Timișoara, Romania
[2] Physics Faculty, University of Bielefeld, Germany

PRD **105** (2022) 014031, WIP

TIM-2022, Timișoara, Romania

Universitatea de Vest din Timişoara

Outline

Introduction

Initial state and observables

Pre-equilibrium evolution

Systems with transverse profiles

Conclusions

Quark-gluon plasma

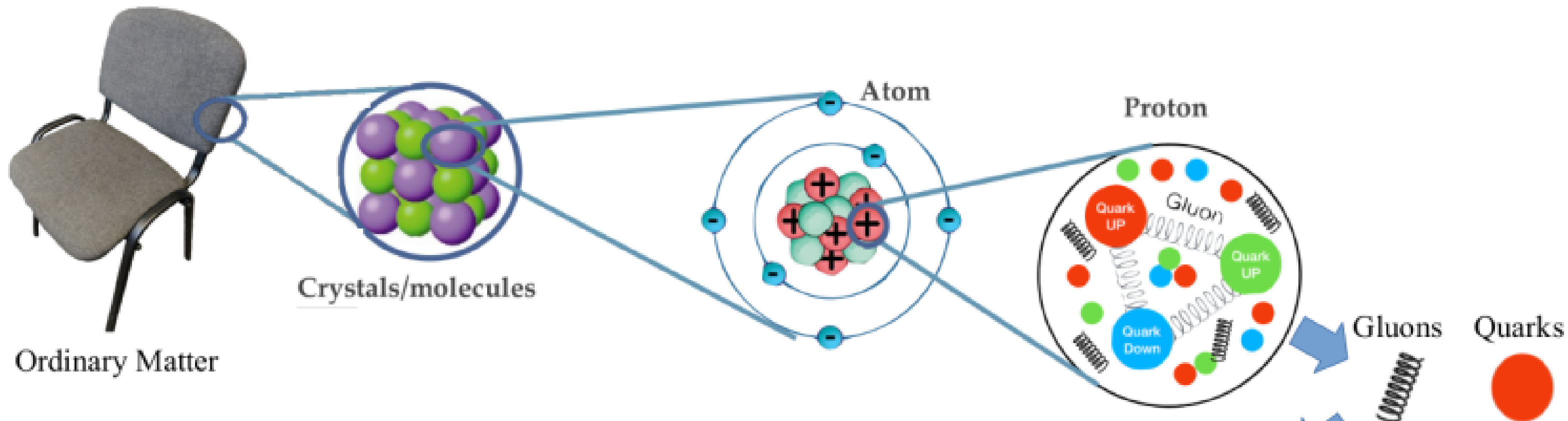

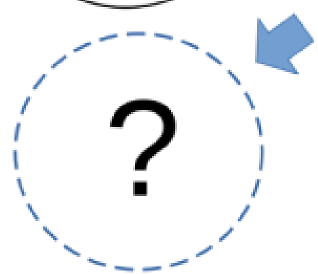

- Quarks are elementary particles interacting via the strong force, mediated by gluons.
- In normal conditions, they exist in bound, colour-neutral configurations (hadrons).
- In extreme conditions ($T \gtrsim 150$ MeV$/k_B \simeq 2 \times 10^{12}$ K), q and g become deconfined $\Rightarrow$ colour-neutral QGP with free colour charges.

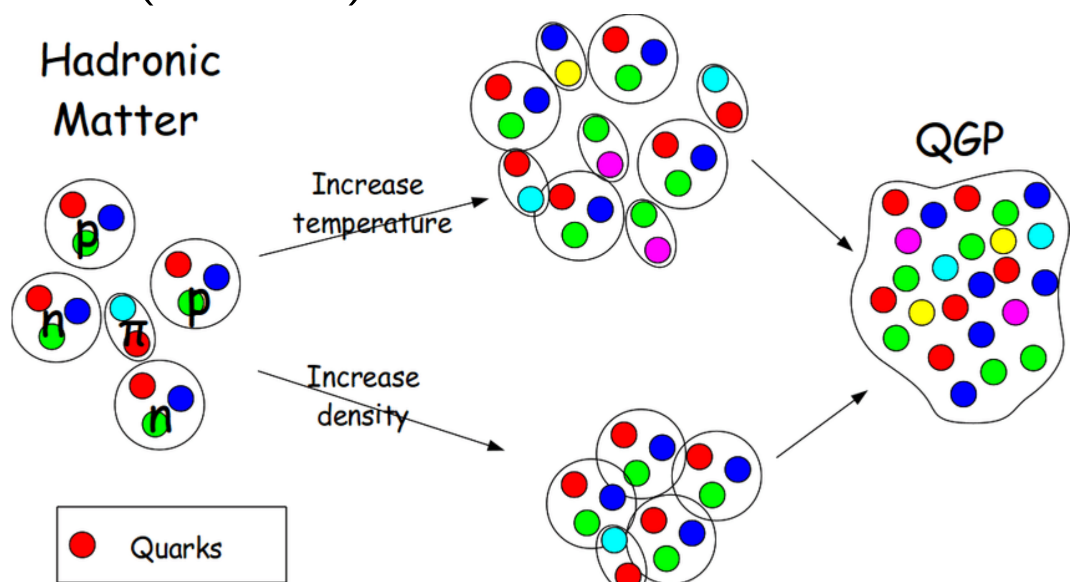

QGP in the laboratory

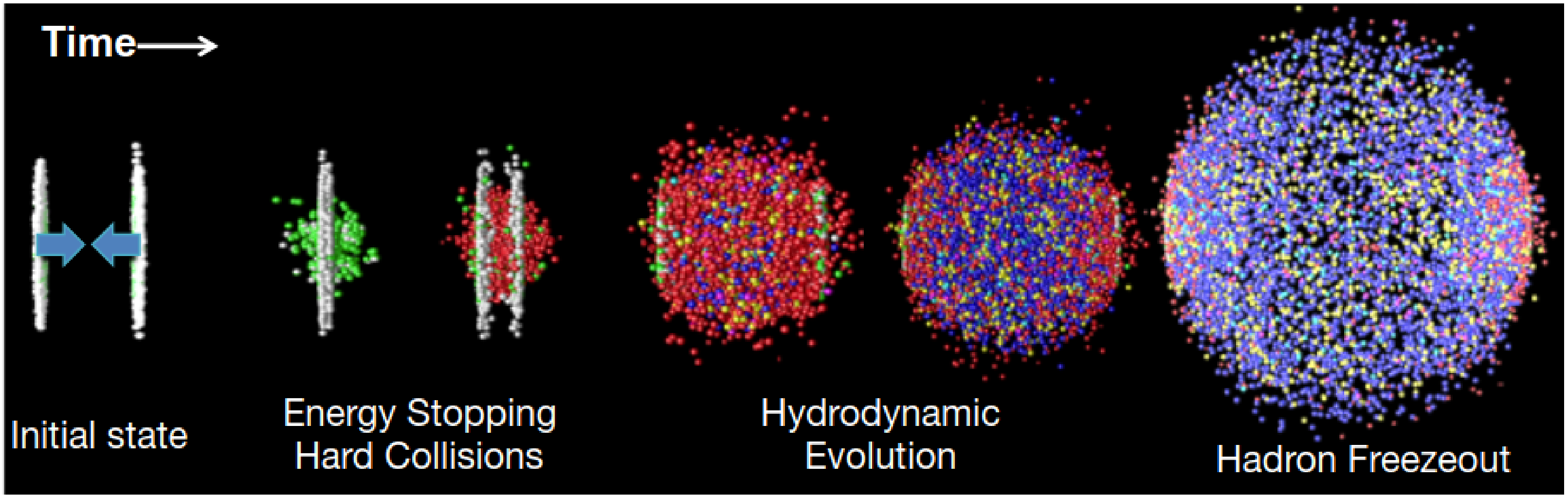

- Bjorken coordinates: $\tau = \sqrt{t^2 - z^2}$; $\eta = \tanh^{-1}(z/t)$.
- Ultra-relatistic heavy-ion collisions ($\sqrt{s_{NN}} = 5.02$ TeV PbPb) deposit $dE_{\perp}/d\eta \sim 1280$ GeV.
- Due to rapid longitudinal expansion, the QGP cools, reaching $k_B T \sim 350$ MeV at $\tau \simeq 1$ fm$/c$.

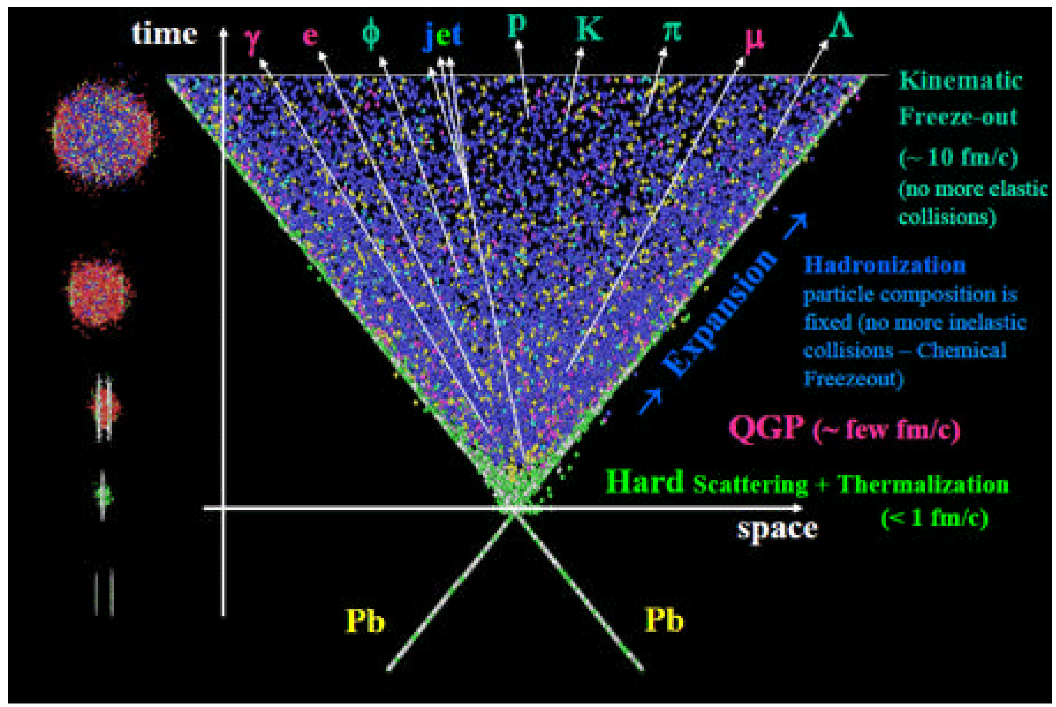

[M. Venaruzzo, PhD Thesis, 2011]

Transverse plane observables

[CMS webpage]

- The overlap region between the colliding nuclei also expands in the transverse plane.
- The strong coupling of the QGP leads to hydrodynamic-like behaviour.
- Initial eccentricities ϵ_n lead to momentum-space anisotropies, characterized by flow harmonics v_n.
- $v_2 \equiv$ elliptic flow was one of the first exp. signatures for the formation of the QGP medium.

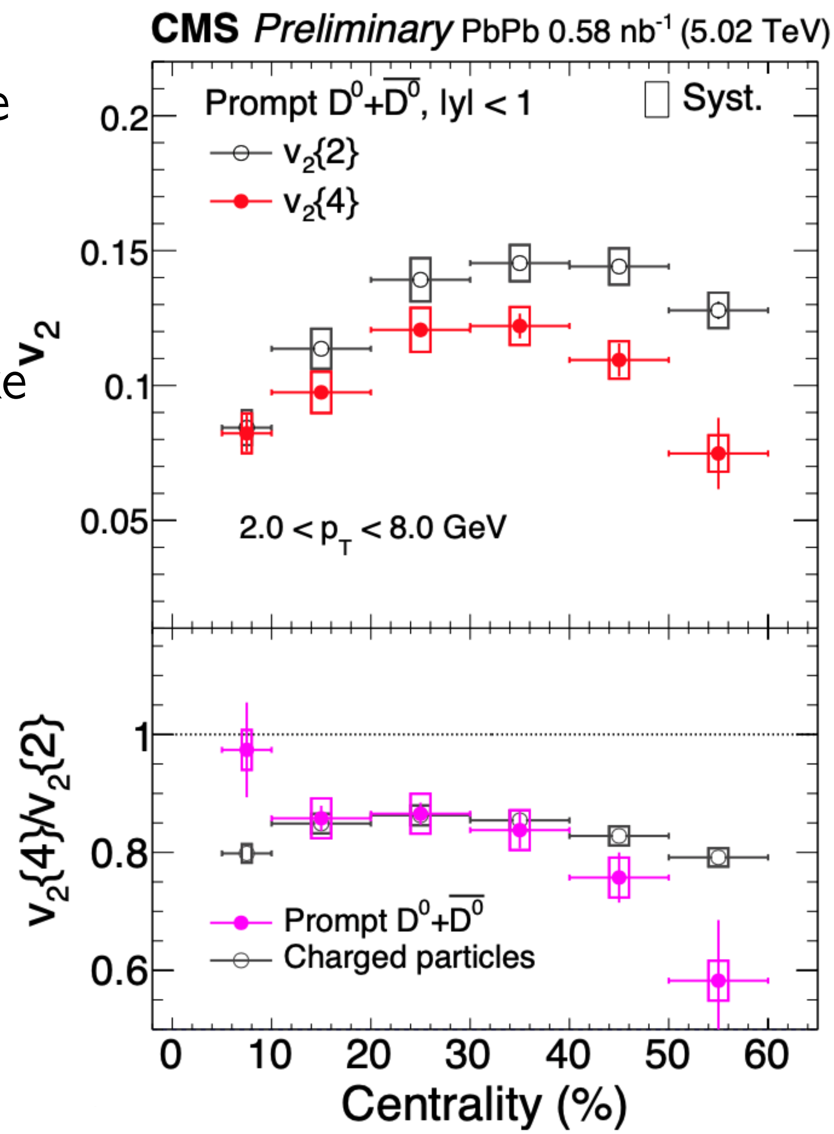

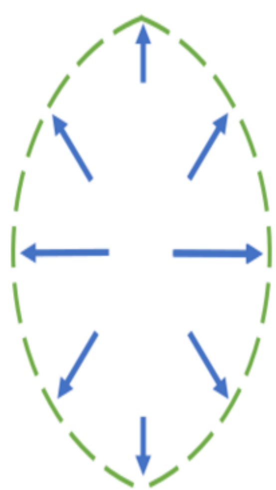

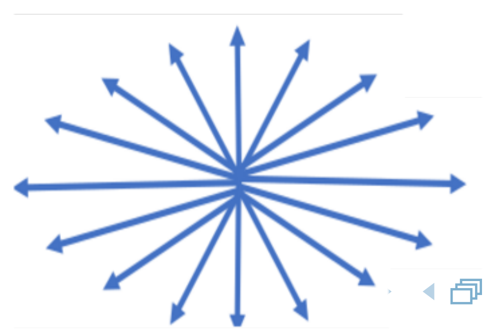

[CMS webpage]

Hadronic Collisions in Experiment

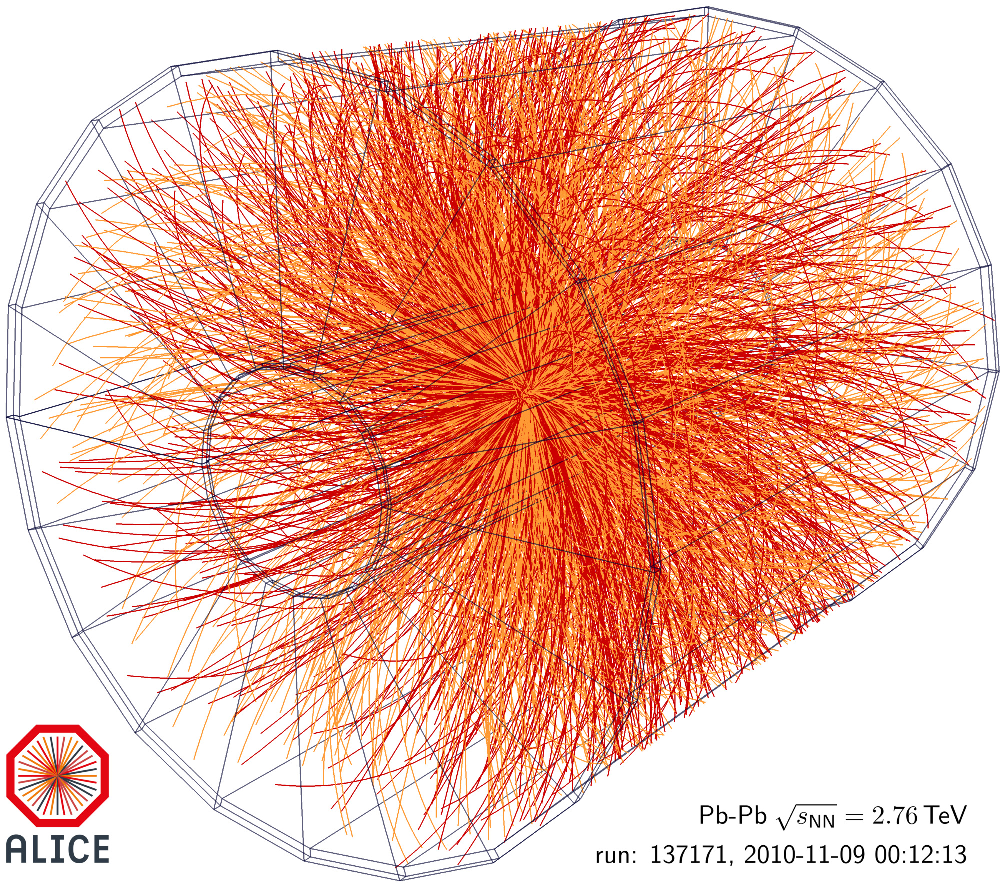

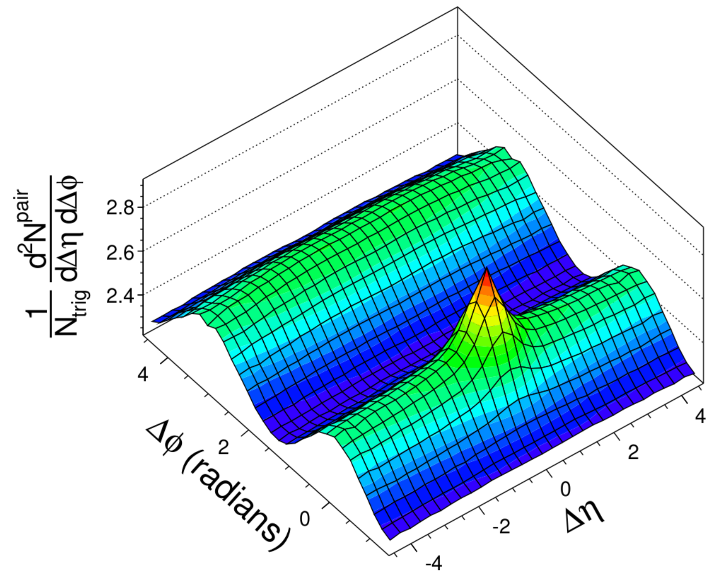

Figure (cropped): CMS Collaboration PLB 724 (2013) 213

Aims of our Work

- Describe spacetime evolution of QCD fireball created in a hadronic collision
- Examine how pre-equilibrium dynamics affects final-state observables (energy $dE_\perp/dy$, Fourier coefficients v_n)
- small densities, large gradients: hydro not necessarily applicable; alternative: microscopic description in terms of kinetic theory
- numerical transport codes simulate these dynamics quite well

AMPT: He, Edmonds, Lin, Liu, Molnar, Wang [PLB 753 (2016) 506]

BAMPS: Greif, Greiner, Schenke, Schlichting, Xu [PRD 96 (2017) 091504]

- Employ simplified description in conformal kinetic theory and conformal hydro to understand the effects of pre-equilibrium dynamics on final-state observables in small and large systems.

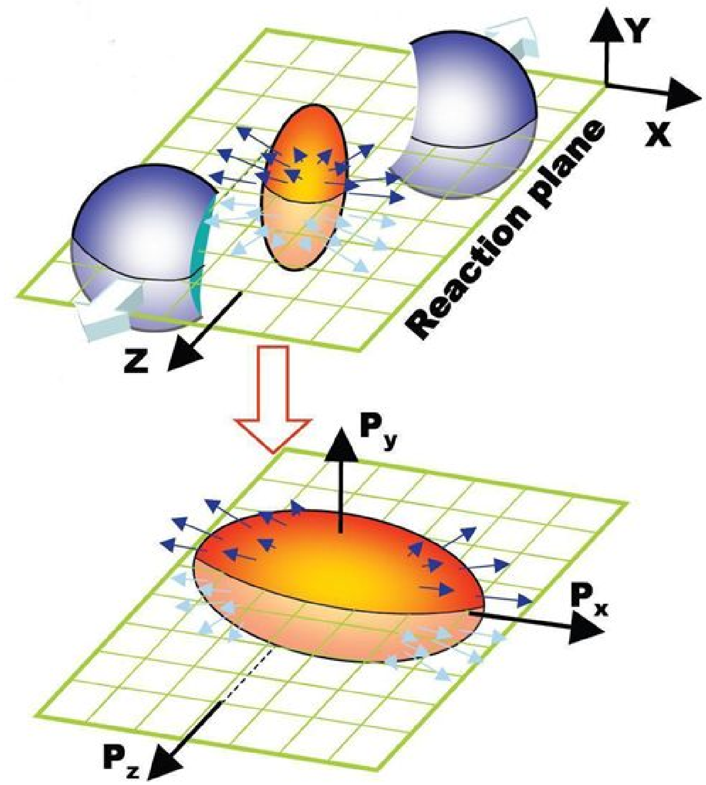

Hiroshi Masui (2008)

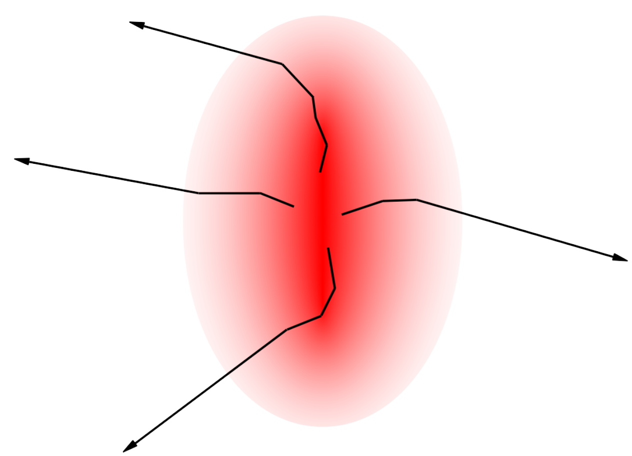

Microscopic description: Kinetic theory (RTA)

- We employ the averaged on-shell phase-space distribution f:

$$f(\tau, \mathbf{x}_\perp, \eta, \mathbf{p}_\perp, y) = \frac{(2\pi)^3}{\nu_{\rm eff}} \frac{dN}{d^3x\, d^3p}(\tau, \mathbf{x}_\perp, \eta, \mathbf{p}_\perp, y). \qquad (1)$$

- For simplicity, we assume boost invariance: $(2+1)+3$D description.
- Time evolution of f governed by Boltzmann eq. in RTA:

$$p^\mu \partial_\mu f = C_{RTA}[f] = -\frac{p_\mu u^\mu}{\tau_R}(f - f_{eq}), \qquad \tau_R = \frac{5\eta/s}{T}, \qquad (2)$$

where the specific shear viscosity $\eta/s \simeq \text{const}$.

- Numerical solution: Relativistic lattice Boltzmann (RLB) method.

[PRC 98 (2018) 035201; PRD 104 (2021) 094022; PRD 105 (2022) 014031]

Macroscopic description: Müller-Israel-Stewart hydro

- Writing $T^{\mu\nu} = (\epsilon + P)u^\mu u^\nu - Pg^{\mu\nu} + \pi^{\mu\nu}$, $\partial_\mu T^{\mu\nu} = 0$ leads to

$$\dot{\epsilon} + (\epsilon + P)\theta - \pi^{\mu\nu}\sigma_{\mu\nu} = 0, \tag{3a}$$

$$(\epsilon + P)\dot{u}^\mu - \nabla^\mu P + \Delta^\mu{}_\lambda \partial_\nu \pi^{\lambda\nu} = 0, \tag{3b}$$

  where $\theta = \partial_\mu u^\mu$ and $\sigma_{\mu\nu} = \nabla_{\langle\mu} u_{\nu\rangle}$.
- In ideal hydro, $\pi^{\mu\nu} = 0$.
- In MIS viscous hydro, $\pi^{\mu\nu}$ evolves according to

$$\tau_\pi \dot{\pi}^{\langle\mu\nu\rangle} + \pi^{\mu\nu} = 2\eta\sigma^{\mu\nu} + \text{h.o.t.} \tag{3c}$$

- Numerical solution obtained using vHLLE.

[Karpenko, Huovinen, Bleicher, CPC 185 (2014) 3016]

Initial state $(\tau_0 \to 0)$

[Borghini, Borrell, Feld, Roch, Schlichting, Werthmann, arXiv: 2209.01176]

30-40% centrality:

Single event:

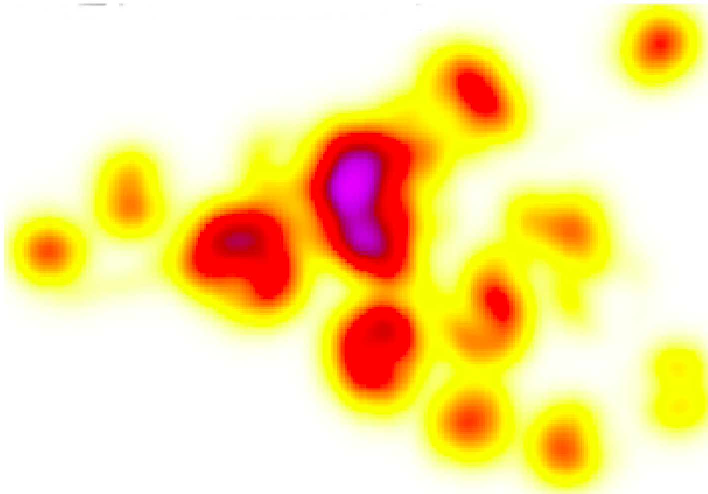

Averaged:

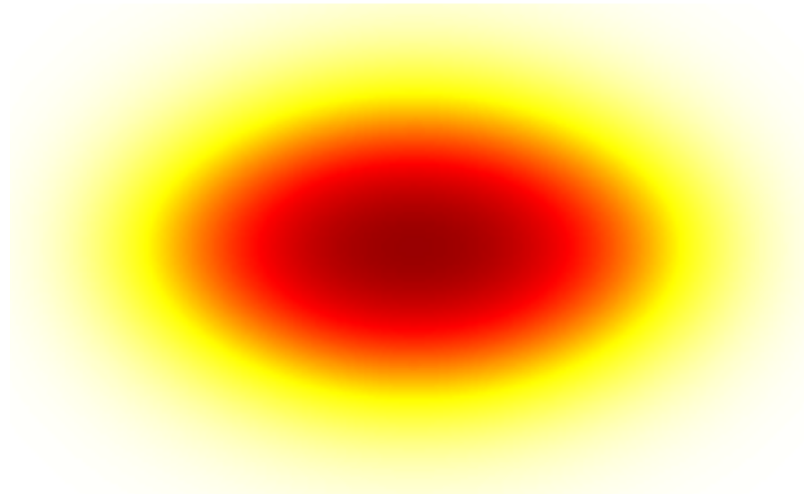

- We consider the initial $dE_\perp^0/d\eta d^2\mathbf{x}_\perp$ for averaged $30-40\%$ centrality PbPb collisions at $5.02\ \mathrm{TeV}$, characterized by

$$\frac{dE_\perp^0}{d\eta} = 1280\ \mathrm{GeV}, \qquad R = 2.78\ \mathrm{fm},$$
$$\epsilon_2 = 0.42, \quad \epsilon_4 = 0.21, \quad \epsilon_6 = 0.09. \qquad (4)$$

Final-state observables ($\tau = 4R$)

- In order to facilitate the comparison between RTA and hydro, we choose final-state observables computable directly from $T^{\mu\nu}$.
- As a proxy for $dE_\perp/d\eta$, we consider

$$\frac{dE_{\text{tr}}}{d\eta} = \tau \int_{\mathbf{x}_\perp} (T^{xx} + T^{yy}). \tag{5}$$

- Similarly, we characterize the flow ellipticity v_2 via

$$\varepsilon_p e^{2i\Psi_p} = \frac{\int_{\mathbf{x}_\perp} (T^{xx} - T^{yy} + 2iT^{xy})}{\int_{\mathbf{x}_\perp} (T^{xx} + T^{yy})}, \tag{6}$$

where Ψ_p is an event-plane angle.

Standard model of heavy-ion collisions

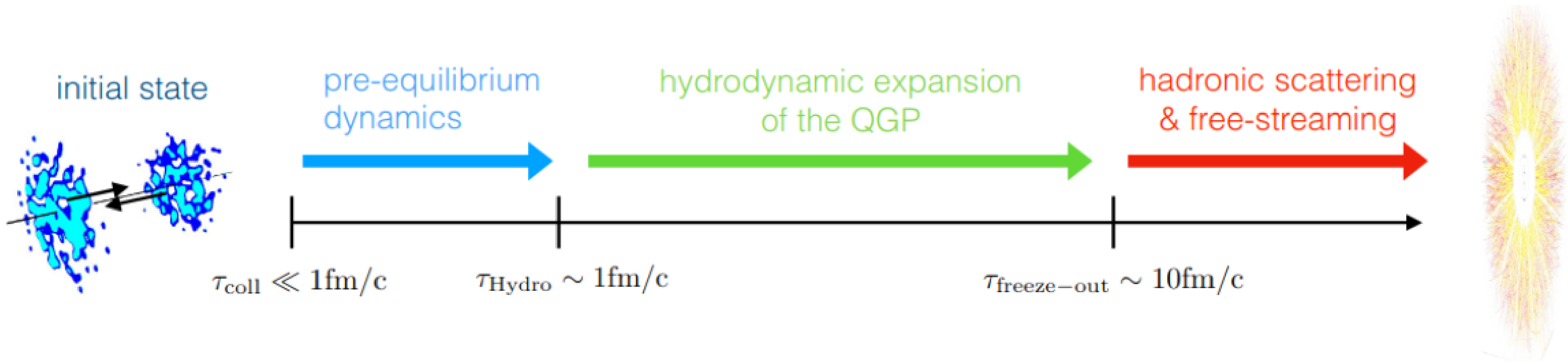

- $\tau_{\rm coll} \equiv \tau_0 \to 0$ to account for pre-eq. dynamics.
- Initially, the system is strongly off-equilibrium ($P_L \simeq 0$).

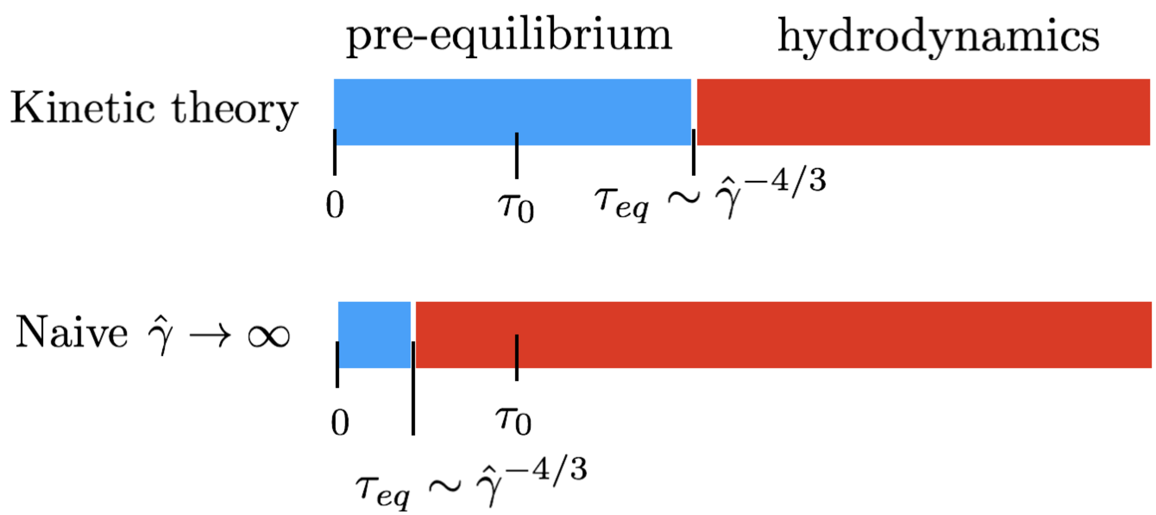

- If $\tau_{\rm Hydro} \equiv \tau_{\rm eq} \lesssim \tau_0$, the pre-eq. phase is not correctly modeled.
- Due to transverse structure, a new time scale R enters the picture
- If $\tau_{\rm eq} \gtrsim R$, equilibration is interrupted by transverse expansion and the system remains off-equilibrium throughout the evolution.

$0 + 1$-D Bjorken flow

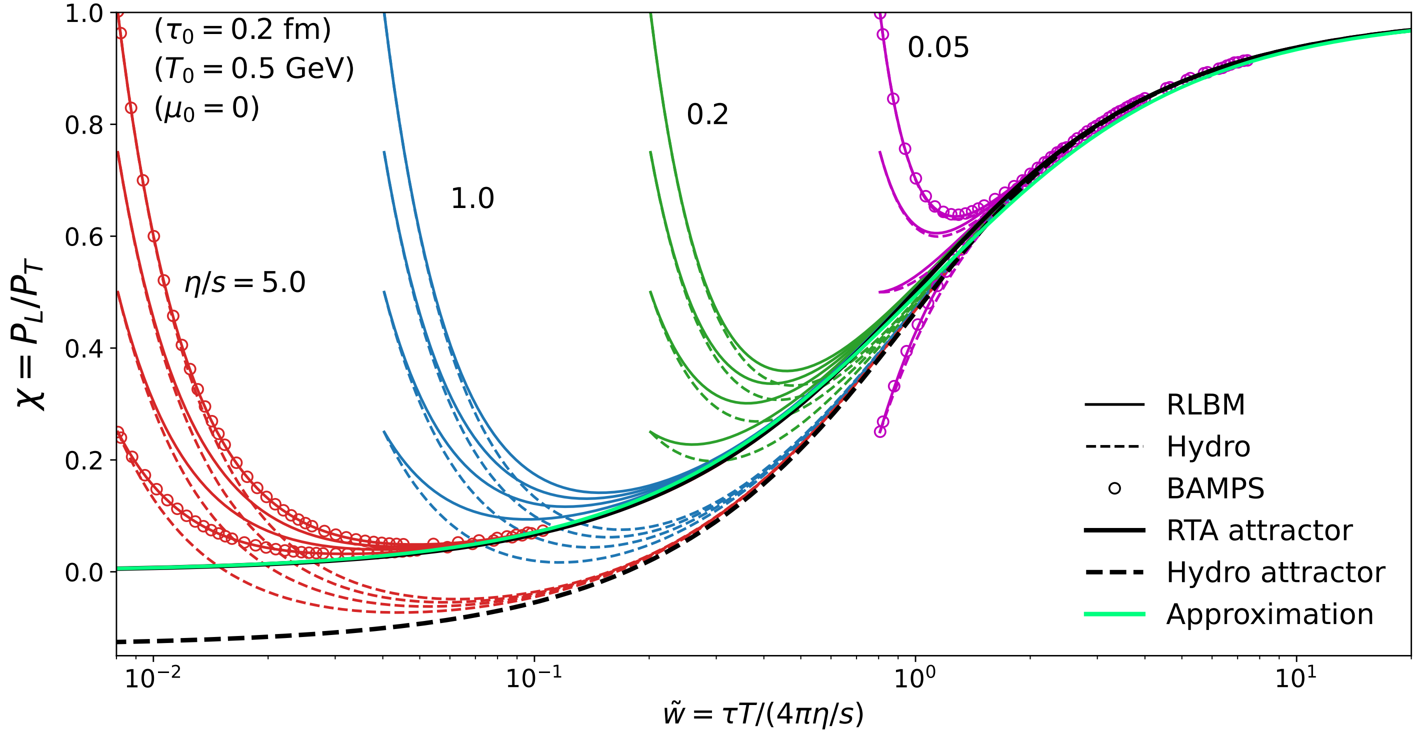

[Ambruș, Bazzanini, Gabbana, Simeoni, Succi, Nature Comput. Sci. **2**, 641 (2022)]

- At early times $\tau \ll R$, transverse expansion is negligible and

$$T^{\mu}{}_{\nu} \simeq \mathrm{diag}(\epsilon, -\mathcal{P}_T, -\mathcal{P}_T, -\mathcal{P}_L),$$
$$\mathcal{P}_T = P - \pi_d/2, \qquad \mathcal{P}_L = P + \pi_d. \tag{7}$$

- $\epsilon = 3P$ evolves according to $\tau \dfrac{\partial(\tau^{4/3}\epsilon)}{\partial\tau} + (\tau^{4/3}\epsilon) f_\pi = 0.$
- $f_\pi = \pi_d/\epsilon$ exhibits attractor behaviour.

[Heller, Spaliński, PRL 115 (2015) 072501]

Scaling solutions

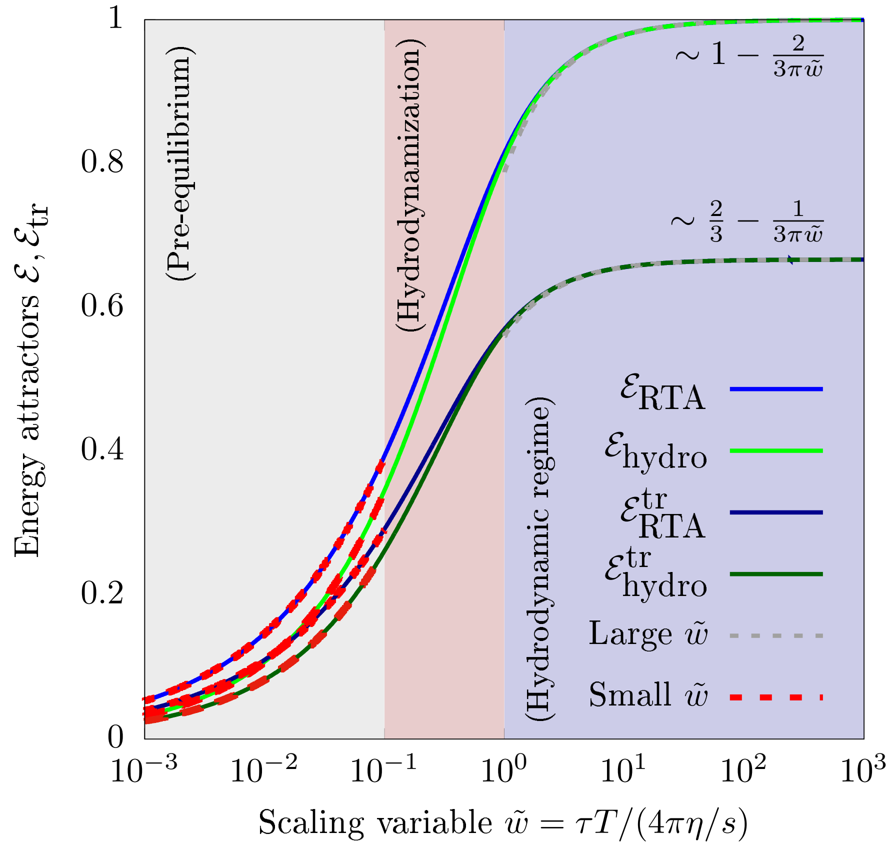

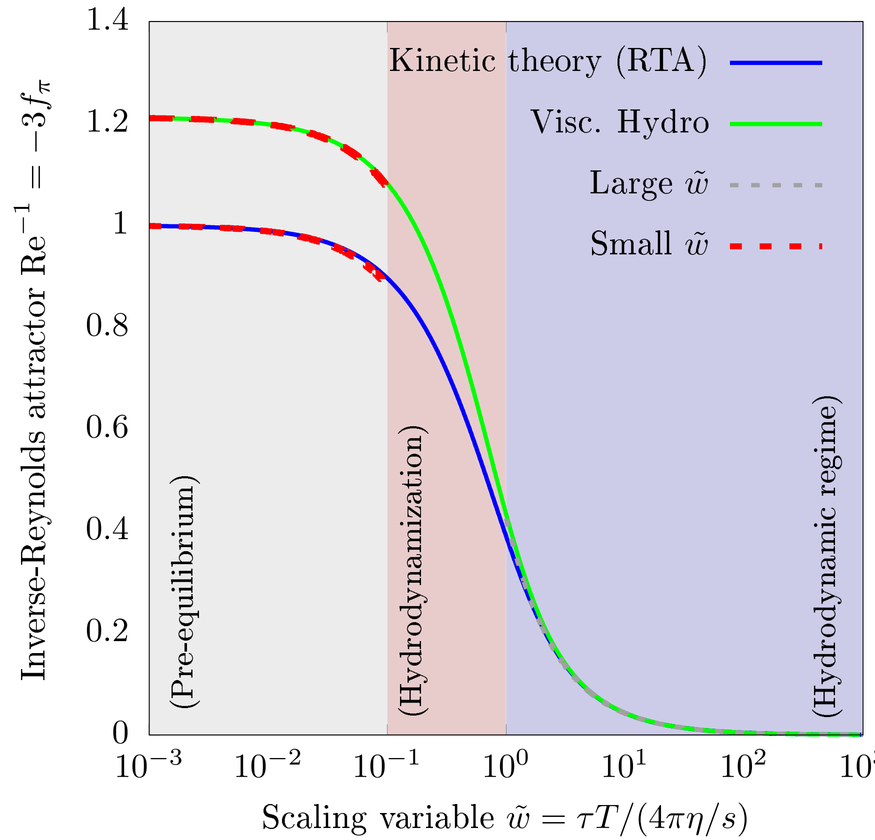

- Along the attractor, f_π and $\tau^{4/3}\epsilon$ are given by

$$f_\pi \equiv f_\pi(\tilde{w}), \qquad \tau^{4/3}\epsilon = \frac{\tau_0^{4/3}\epsilon_0}{\mathcal{E}(\tilde{w}_0)}\mathcal{E}(\tilde{w}), \tag{8}$$

where $\tilde{w} = \dfrac{\tau T}{4\pi\eta/s}$ is the scaling variable.

Pre-equilibrium dynamics ($\tilde{w} \ll 1$)

- Around $\tilde{w} = 0$ (FS fixed point), f_π and $\mathcal{E}$ behave like

$$f_\pi(\tilde{w} \ll 1) \simeq f_{\pi;0}, \\ \mathcal{E}(\tilde{w} \ll 1) \simeq C_\infty^{-1} \tilde{w}^\gamma, \tag{9}$$

  where the constants $f_{\pi;0}$, γ and C_∞ depend on the theory:

$$\gamma_{\rm RTA} = \frac{4}{9}, \qquad \gamma_{\rm hydro} = \frac{1}{18}(\sqrt{505} - 13) \simeq 0.526. \tag{10}$$

- When Eq. (9) applies, we have

$$\epsilon(\tilde{w} \ll 1) \simeq \left(\frac{\tau_0}{\tau}\right)^{(\frac{4}{3} - \gamma)/(1-\gamma/4)} \epsilon_0. \tag{11}$$

- In RTA: $\tau\epsilon \simeq \text{const.}$
- In hydro: $\tau\epsilon \propto \tau^{0.07}$ increases with time.

Scaled hydrodynamics

- At $\tilde{w} \gg 1$, the RTA and hydro attractors agree:

$$\mathcal{E}(\tilde{w} \gg 1) = 1 - \frac{2}{3\pi\tilde{w}}.$$

- We scale hydro such that $(\tau^{4/3}\epsilon)^{\text{hydro}}_{\infty} = (\tau^{4/3}\epsilon)^{\text{RTA}}_{\infty}$:

$$C^{\text{hydro}}_{\infty} \frac{\epsilon_0^{\text{hydro}}}{\tilde{w}_0^{\gamma}} = C^{\text{RTA}}_{\infty} \frac{\epsilon_0^{\text{RTA}}}{\tilde{w}_0^{4/9}}.$$

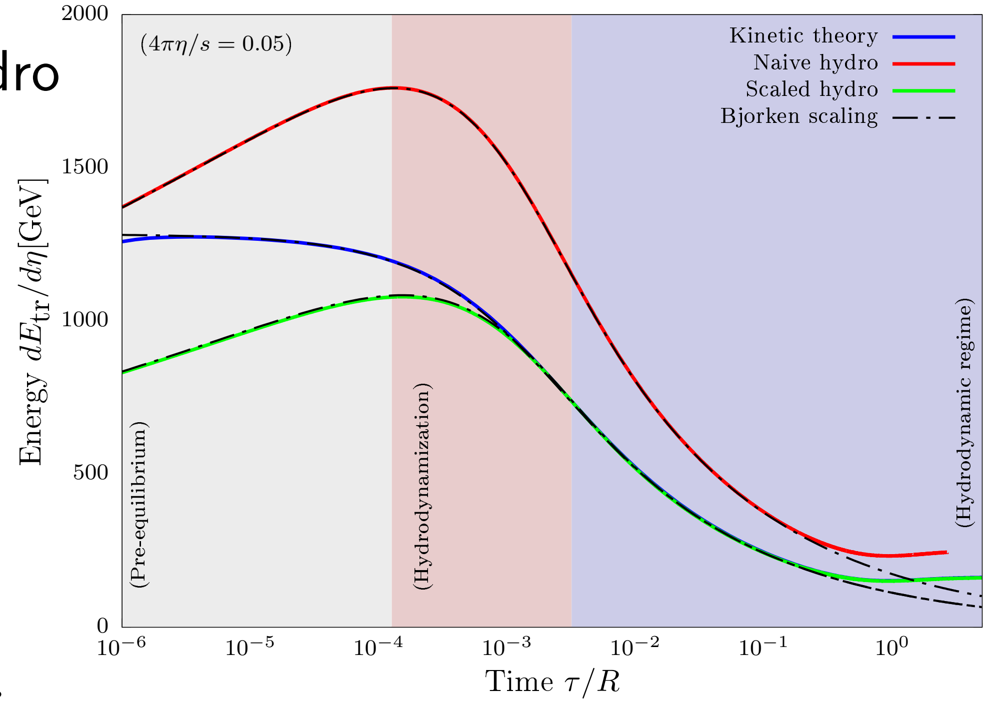

- Taking into account that $\tilde{w}_0 = \tau_0 T_0/(4\pi\eta/s)$ and $T_0 = (\epsilon_0/a)^{1/4}$, the solution is

$$\epsilon_0^{\text{hydro}} = \left[\left(\frac{4\pi\eta/s}{\tau_0} a^{1/4} \right)^{\frac{1}{2} - \frac{9\gamma}{8}} \left(\frac{C^{\text{RTA}}_{\infty}}{C^{\text{hydro}}_{\infty}} \right)^{9/8} \epsilon_0^{\text{RTA}} \right]^{\frac{8/9}{1-\gamma/4}}. \quad (12)$$

Final state ($\tau = 4R$): Transverse energy $dE_{\rm tr}/d\eta$

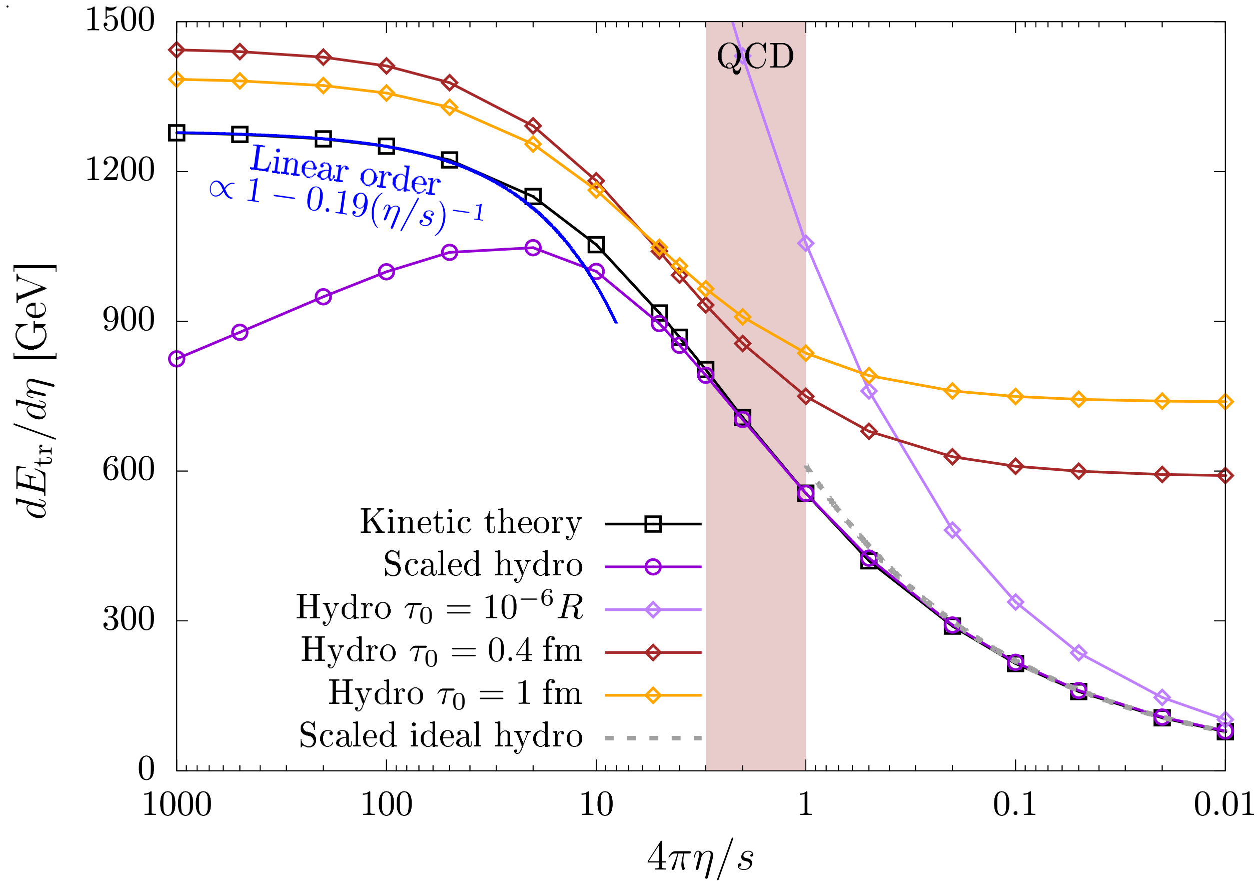

- [Naive hydro, small η/s] Larger $\tau_0 \Leftrightarrow$ larger final-state value, since late-time $dE_{\rm tr}/d\eta \propto \tau^{-1/3}$ decrease lasts less.
- [Naive hydro, large η/s] Smaller $\tau_0 \Leftrightarrow$ larger $dE_{\rm tr}/d\eta$ due to pre-eq. increase.
- [Scaled hydro, small η/s] Works well for $4\pi\eta/s \lesssim 3$.
- [Scaled hydro, large η/s] Transverse expansion interrupts pre-eq. $\Rightarrow dE_{\rm tr}/d\eta$ doesn't increase sufficiently to match RTA.

Inhomogeneous cooling and scaled eccentricity

- For $\tau \lesssim 0.1R$, the system evolves as a collection of $0+1$-D Bjorken flows $\Rightarrow$ inhomogeneous cooling.
- If $\tilde{w} \gtrsim 1$ when $\tau \sim R$, equilibration occurs before transverse expansion sets in and late-time limits governed by

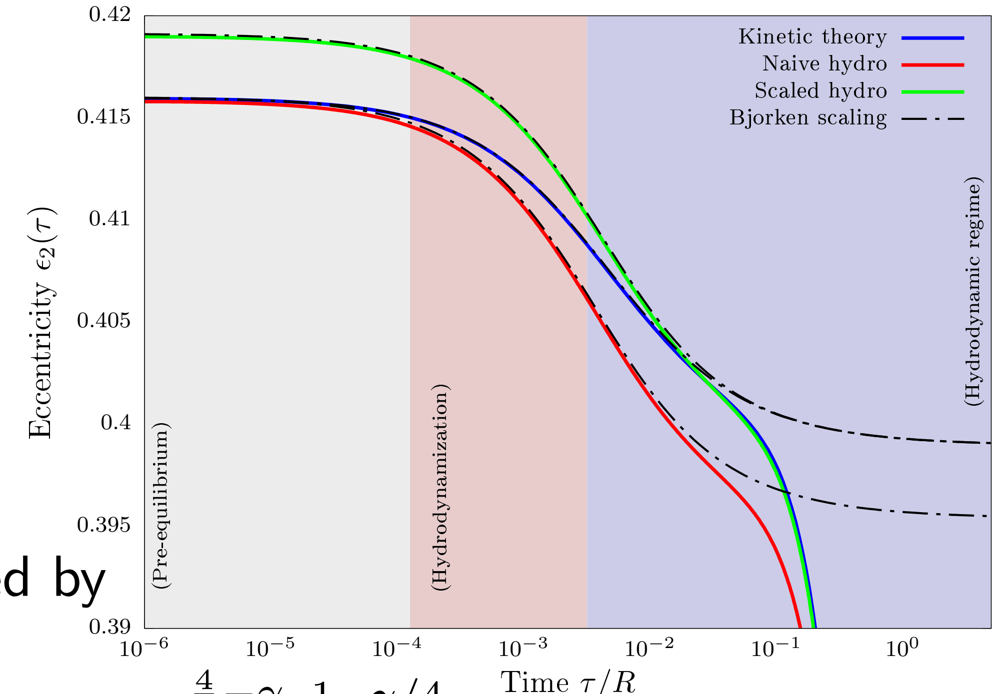

$$(\tau^{4/3}\epsilon)_\infty \propto \tau_0^{\frac{4}{3}-\gamma}\epsilon_0^{1-\gamma/4}. \tag{13}$$

- The eccentricity $\epsilon_2 = (\int_{\mathbf{x}_\perp}\epsilon)^{-1}\int_{\mathbf{x}_\perp}\epsilon x_\perp^2\cos(2\phi)$ changes according to

$$\epsilon_n \simeq \left(\int_{\mathbf{x}_\perp}\epsilon_0^{1-\gamma/4}\right)^{-1}\int_{\mathbf{x}_\perp}\epsilon_0^{1-\gamma/4}x_\perp^2\cos(2\phi). \tag{14}$$

- The exponent $1-\frac{\gamma}{4}$ implies that ϵ_2 changes differently in hydro compared to RTA $\Rightarrow$ scaled hydro changes initial ϵ_2 s.t. $\lim_{\tau\to\infty}\epsilon_2^{\text{hydro}} = \lim_{\tau\to\infty}\epsilon_2^{\text{RTA}}$.

Final state ($\tau = 4R$): Elliptic flow ε_p

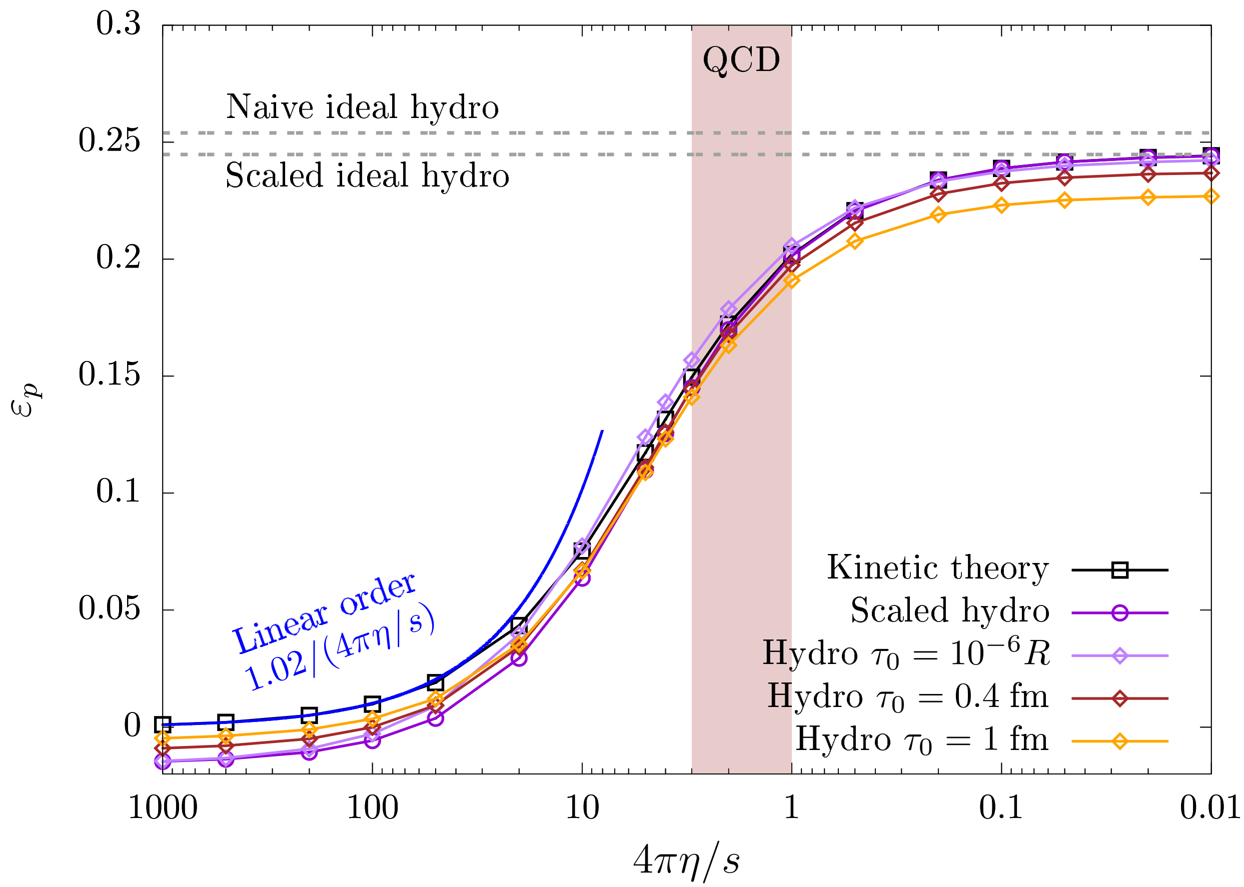

- [Naive hydro, small η/s] Remains in disagreement with naive ideal hydro. Approach to RTA: lucky coincidence?
- [Scaled hydro, small η/s] In excellent agreement with scaled ideal hydro & RTA.
- [Hydro, large η/s] Pre-equilibrium in hydro leads to negative build-up of ε_p (less for larger τ_0), which persists at late times (in contrast to RTA).

Conclusions

- Bjorken $0+1$-D attractor governs the system's evolution for $\tau \lesssim 0.1R$.
- Differences in the early-time behaviour of hydro and RTA lead to discrepancies in final-state observables.
- Agreement between RTA and hydro is restored at small η/s by scaling the initial conditions for hydro in order to balance the pre-equilibrium differences.
- For the sample $30-40\%$ centrality class of $\mathrm{Pb}-\mathrm{Pb}$ collisions at $\sqrt{s_{NN}} = 5.02$ TeV, scaled hydro provides a reasonable description when $4\pi\eta/s \lesssim 3$.
- Possible improvements include hybrid schemes: kinetic theory for pre-equilibrium and equilibration and hydro for the rest.
- This work was supported through a grant of the Ministry of Research, Innovation and Digitization, CNCS - UEFISCDI, project number PN-III-P1-1.1-TE-2021-1707, within PNCDI III.